Composites: Part B 60 (2014) 350–358

Contents lists available at ScienceDirect

Composites: Part B

journal homepage: www.elsevier.com/locate/compositesb

Mechanical behaviors of carbon fiber composite sandwich columns with three dimensional honeycomb cores under in-plane compression

Jian Xiong [a,*], Meng Zhang [a], Ariel Stocchi [b], Hong Hu [c], Li Ma [a], Linzhi Wu [a,*], Zhong Zhang [d]

[a] Center for Composite Materials and Structures, Harbin Institute of Technology, Harbin 150001, China
[b] Research Institute of Material Science and Technology (INTEMA), National University of Mar del Plata (UNMdP), Mar del Plata, Argentina
[c] Institute of Textiles and Clothing, The Hong Kong Polytechnic University, China
[d] Science and Technology on Reliability and Environment Engineering Laboratory, Beijing Institute of Structure and Environment Engineering, Beijing 100076, China

ARTICLE INFO

Article history:
Received 9 August 2013
Received in revised form 28 October 2013
Accepted 22 December 2013
Available online 31 December 2013

Keywords:
A. Honeycomb
B. Mechanical properties
C. Analytical modelling
D. Mechanical testing

ABSTRACT

Mechanical properties and failure modes of carbon fiber composite egg and pyramidal honeycombs cores under in plane compression were studied in the present paper. An interlocking method was developed for both kinds of three-dimensional honeycombs. Euler or core shear macro-buckling, face wrinkling, face inter-cell buckling, core member crushing and face sheet crushing were considered and theoretical relationships for predicting the failure load associated with each mode were presented. Failure mechanism maps were constructed to predict the failure of these composite sandwich panels subjected to in-plane compression. The response of the sandwich panels under axial compression was measured up to failure. The measured peak loads obtained in the experiments showed a good agreement with the analytical predictions. The finite element method was used to investigate the Euler buckling of sandwich beams made with two different honeycomb cores and the comparisons between two kinds of honeycomb cores were conducted.

1. Introduction

Cellular structures have been available for decades due to high stiffness and strength [1–3]. A broad range of materials were employed over the years in cellular cores construction, such as aluminum alloys [4–6], steel wires [7], polymers [8], self-propagating polymers [9], hollow-tube micro lattices [10], and Kraft paper [11]. Fiber reinforced composites [12,13] have provided even a greater flexibility to novel sandwich structures for their adaptation to several operating conditions and design restrictions. The inner spaces of the traditional foam and honeycomb cores restrict the circulation of a flow inside the sandwich panel, thus its application in functional structures is limited [14]. Therefore, open-cell cores with interconnected void spaces were suggested to manufacture sandwich panels for functional applications rather than as load-bearing structures [15]. The dynamic behavior of square honeycomb cores was studied by Ebrahimi and Vaziri [16] and Vaziri and Hutchinson [17]. Xin and Lu [18,19] investigated the sound radiation and transmission of square honeycomb cores. Fan et al. [20,21] first studied the out-of-plane compression, in-plane compression and bending response of Kagome grid cores, and then developed hierarchical lattice composites for mechanical energy absorptions based on interlocking method [22,23]. Russell et al. [24,25] and Park et al. [26] investigated the out-of-plane compression and bending responses of square honeycomb cores. Ajdari et al. [27,28] reported the dynamic crushing and energy absorption of 2D cellular structures. Petrone et al. [29] investigated the mechanical behavior of honeycomb core panels made from natural fiber. To date, the existing literature on honeycomb cores is mainly concerned with the out-of-plane compression, dynamic, shear and bending performance, and the in-plane compressive response has only received limited attention. However, in satellite [30] and crashworthiness applications [31], for example, plane compression is a very common solicitation. Since 2D honeycomb cores are made with close cells, they can mainly be used as loading bearing structures. Therefore, their multifunctional benefit is very limited. To overcome this deficiency, three-dimensional (3D) carbon fiber reinforced honeycomb cores, which combine the advantages of both 2D honeycombs and hollow cores with interconnected void spaces, can be a better choice. In this work, these kinds of structures were developed. An inherent part of this study is a need to understand the mechanical behavior of this novel structure. Since the core crushing behavior and out-of-plane compressive response of the 3D honeycomb panel were studied in our previous work [32], the response of carbon fiber composite sandwich beam with three dimensional honeycomb cores subjected to in-plane compression is the focus of the present work. Analytical expressions

* Corresponding authors. Tel.: +86 451 86412549; fax: +86 451 86402386.
E-mail addresses: jx@hit.edu.cn (J. Xiong), wlz@hit.edu.cn (L. Wu).

1359-8368/$ - see front matter © 2014 Elsevier Ltd. All rights reserved.
http://dx.doi.org/10.1016/j.compositesb.2013.12.049

for the failure load of composite sandwich columns under in-plane compression were derived by expanding the previous analytical work on metal and carbon fiber sandwich columns with pyramidal truss cores [33–35] and sandwich columns made of carbon fiber reinforced epoxy face sheets with honeycomb cores [36]. Failure mechanism maps were constructed with four competing failure modes. Face sheets with three different layer stacking were investigated and the relationship between the failure mechanism maps and material mechanical properties was discussed. The finite element method was also used to investigate the Euler buckling of sandwich beam which cannot be observed during tests. Although the investigation of this work only focused on the mechanical properties and failure mechanisms of sandwich columns with 3D honeycomb cores, the obtained results and analysis methods could be extrapolated for the development of other lightweight and multifunctional sandwich structures.

2. Experimental

2.1. Materials and fabrication

A method for fabricating carbon fiber composite egg and pyramidal honeycomb cores for in-plane compression is presented in this section. The plate interlocking method used to form the honeycomb sandwich columns is shown in Fig. 1. First, 0°/90° carbon fiber composite laminates were made with 0.15 mm thick T700/epoxy prepreg (T700/epoxy composite, Beijing Institute of Aeronautical Materials, China). The properties of the unidirectional prepreg used are provided in Table 1. Each plate was interlocked with other plate only from the long caulking groove to form egg lattice cores, and each plate interlocked with other plates including both long and short caulking grooves to form pyramidal lattice cores. The details of the interlocking methods could be found in [32]. The fabricated egg and pyramidal honeycomb sandwich structures are sketched in Figs. 2 and 3, respectively. Finally, two face sheets were bonded on the top and bottom of the honeycomb core to obtain a sandwich column and both ends are filled with epoxy resin.

An approximation of the relative density of the egg honeycombs' core can be made with the following equation:

$$\bar{\rho} = \frac{d[(b+a-2t)(H-h)+2ah-d]}{a^2 H} \quad (1)$$

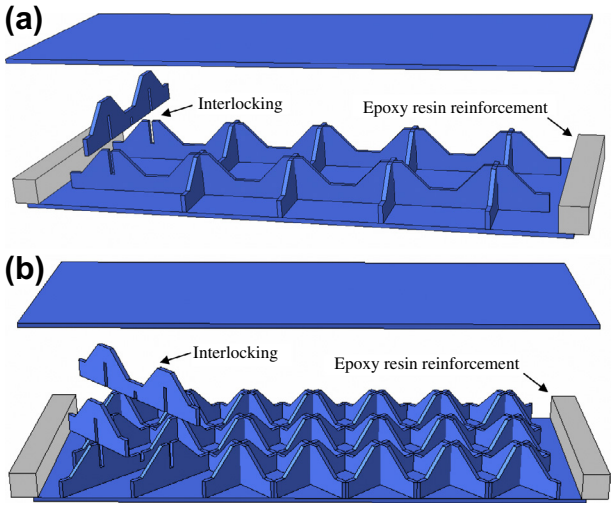

Fig. 1. Fabrication of sandwich columns with 3D honeycomb cores for in-plane compressive tests by using cut carbon fiber reinforced composite sheets and interlock method: (a) egg honeycomb cores and (b) pyramidal honeycomb cores.

Table 1
Properties of unidirectional lamella (T700/epoxy composites).

Properties	Value
0° Tensile strength (MPa)	1400
0° Tensile modulus (GPa)	123
90° Tensile strength (MPa)	18
90° Tensile modulus (GPa)	8.3
0° Compression strength (MPa)	850
0° Compression modulus (GPa)	100
90° Compression strength (MPa)	96
90° Compression modulus (GPa)	8.4
In-plane shear strength (MPa)	16.0
In-plane shear modulus (GPa)	4.8
Interlayer shear strength (MPa)	60
Poisson's ratio	0.3
Volume fraction of fibers	57% ± 3
Density (kg/m^3)	1550

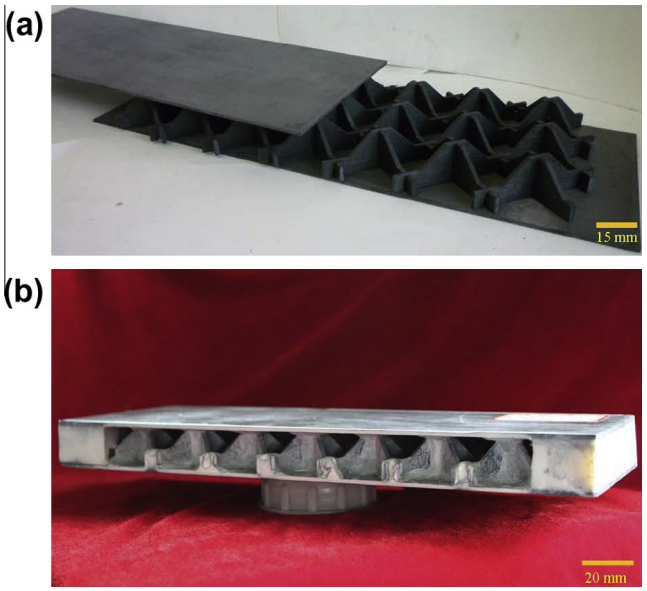

Fig. 2. Photographs of pramidal honeycomb sandwich structures (a) and specimen ($\bar{\rho} = 12.0\%$) for in-plane compression tests (b).

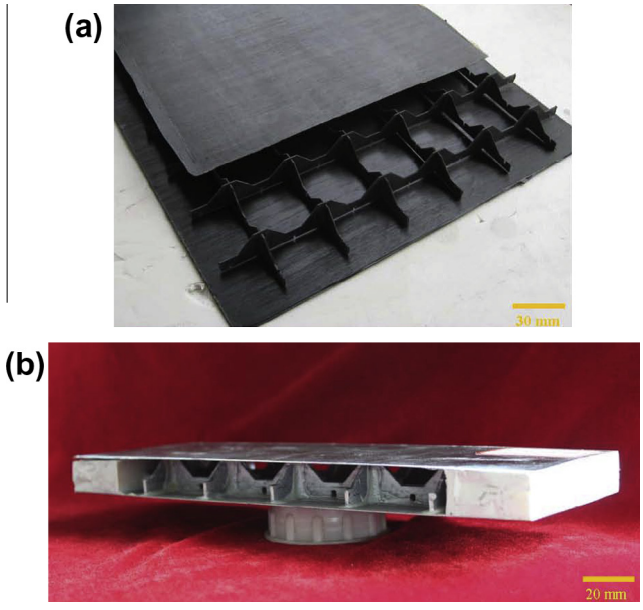

Fig. 3. Photographs of egg honeycomb sandwich structures with $\bar{\rho} = 3.0\%$ (a) and specimen ($\bar{\rho} = 6.0\%$) for in-plane compression tests (b).

where the geometrical parameters, b, H, h, t and d, are shown in the schematic figure of the unit cell of the egg and pyramidal honeycomb structures, as shown in the bottom of Fig. 4(a) and (b), respectively. The relative density of pyramidal honeycomb cores is two times of that of the egg honeycomb cores. All the core relative densities were calculated based on the same thickness of cut plate $d = 2$ mm. The pyramidal honeycomb structure shown in Fig. 2 has $b = 12$ mm, $H = 20$ mm, $h = 8$ mm, $d = 2$ mm. These sandwich structures were fabricated by attaching the pyramidal honeycomb structures to flat carbon fiber reinforced face sheets with adhesive (08-57, Heilongjiang Institute of Petrochemical, China).

2.2. In-plane compressive tests

Fig. 4 shows the experimental setup of egg and pyramidal honeycomb sandwich columns under in-plane compression. The responses of both egg and pyramidal honeycomb core sandwich columns were measured using INSTRON (Norwood, MA, USA) series 5500 following ASTM C365/C 364M-05 standard recommendations. The ends of the panels were first filled with an epoxy resin of length $S = 15$ mm in order to limit local failure, as schematically shown in Figs. 2(b) and 3(b). The axial compression tests were carried out in the quasi-static regime with a nominal displacement rate of 0.5 mm/min. At least two tests were carried out for each column's geometry to ensure the repeatability of the results. Three different specimens were designed for egg and pyramidal honeycomb cores, respectively. Almost all the failure modes mentioned above were found in our tests and several different models could be investigated for the same specimen. The failure for each specimen designed by the failure mechanism maps will be described in the following section. For each failure mechanism map, three different specimens will be designed for both egg and pyramidal honeycomb cores.

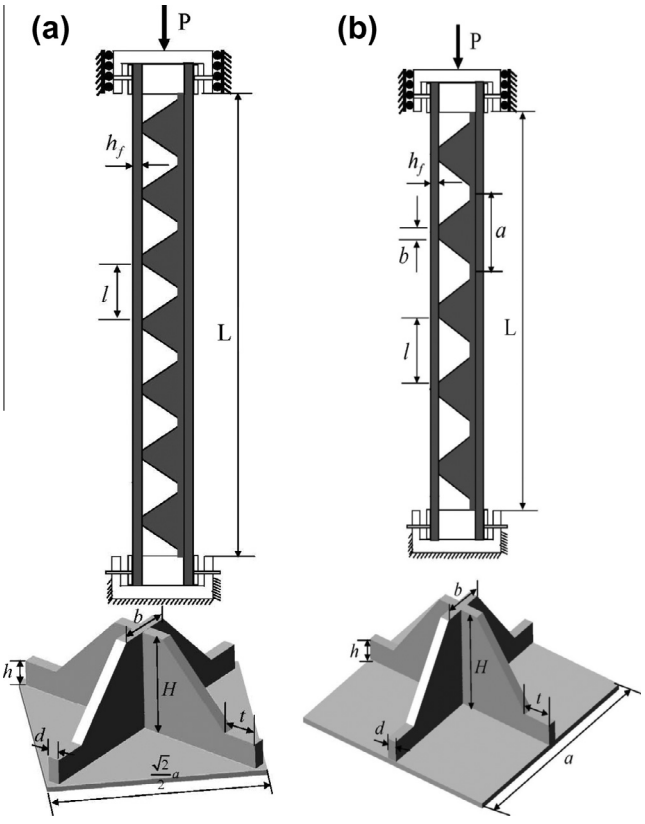

Fig. 4. Schematic diagram of the in-plane compression test assembly and the unit cell of 3D honeycomb cores: (a) pyramidal honeycomb cores and (b) egg honeycomb cores.

3. Analytical predictions for competing failure modes

3.1. Analytical prediction

So far there is no available literature about the mechanical response and failure modes of carbon fiber composite pyramidal or egg honeycomb cores under axial compression. In the following sections, a full range of analytical models were developed in order to predict the failure modes of both 3-D honeycombs cores sandwich columns made by carbon fiber reinforced composite. Four different failure modes were considered: (i) Euler or core shear macro-buckling, (ii) face wrinkling, (iii) face intra-cell buckling, and iv) face crushing including face delamination and plastic micro-buckling.

3.1.1. Euler and core shear macro-buckling

Euler buckling and core shear buckling are two possible modes of elastic macro-buckling in a sandwich panel under axial compression (i.e. buckling modes with wavelength in the order of panel dimensions). The Euler buckling load, P_B, can be estimated from the classical buckling theory [37] as:

$$P_B = \frac{k^2\pi^2(EI)_{eq}}{L^2} \tag{2}$$

where $(EI)_{eq}$ is the equivalent flexural rigidity of the composite column, L is the span length of specimen and $k = 2$ for a column with built-in ends. It is assumed that the Poisson ratios of the core in the in-plane direction are insignificant, in terms of the equivalent flexural rigidity of the composite column [38], as given by:

$$(EI)_{eq} = \frac{wh_fH^2E_f}{2} \tag{3}$$

where E_f is the Young's moduli of the face sheet, h_f is the thickness of the face sheet, H is the height of the core materials and w is the width of the sandwich column.

In studying the core shear buckling, it is reasonable to neglect the shear stiffness of the face sheets and assume that the shear rigidity of the sandwich column is approximately equal to that of the three dimensional honeycombs core. The core shear-buckling load can be obtained based on the method in other work [35].

$$P_S \approx G_cwH \tag{4}$$

where G_c is the effective shear modulus of the three dimensional honeycombs core and can be obtained from the shear tests. If two buckling loads associated with the sandwich panel macro-buckling, P_S and P_B, are considerably different, Eqs. (4) and (6) can be used to estimate the critical buckling load, P_{cr} (i.e. If $P_S \gg P_B$, then $P_{cr} \approx P_B$; if $P_B \gg P_S$, then $P_{cr} \approx P_S$). However, if the Euler and core shear buckling loads are the same order of magnitude, the interaction between buckling modes should be considered. In this case, the critical buckling load can be estimated from, $1/P_{cr} = 1/P_B + 1/P_S$.

3.1.2. Face wrinkling

A sandwich with a honeycomb core may fail by buckling of the face where it is unsupported by the walls of the honeycomb; this being more likely to occur in the weak side of panel. The face sheet of a sandwich panel is generally much stiffer than its low density core, so the strain mismatch between the face sheet and core (here, induced by axial compression) could lead to face sheet instability in the form of wrinkles with a short wavelength. In this work, it was assumed that the face sheets behave elastically and the wavelength of the face wrinkles is equal to the length between the attachment points of three dimensional honeycombs core to the

face sheet, denoted by l in Fig. 4, where $l = \frac{\sqrt{2}}{2}a - b\cos 45^\circ$ for pyramidal honeycomb cores and $l = a - b$ for egg honeycomb cores. The force associated with the elastic wrinkling of the face sheet, P_W, can be estimated from

$$P_W = \frac{a\pi^2 (EI)_f}{l^2} \tag{5}$$

where $(EI)_f$ is the flexural rigidity of the face sheet in relation to the panel mid-plane, which can be obtained using the classical laminate composite beam theory.

3.1.3. Intra-cell buckling

Intra-cell buckling is a local buckling phenomenon which can take place in three dimensional honeycombs core sandwich structures. Intra-cell buckling, also referred as "dimpling" or "inter-cell buckling", is the buckling of the face sheet within an individual honeycomb cell. Although the three dimensional honeycomb structure will preserve part of its load-carrying capacity after intra-cell buckling has occurred, the buckled face sheet may have undesirable influences, for example, it can adversely affect the aerodynamic properties of the structure; thus, it is important to know the load at which this intra-cell buckling occurs. According to the Norris formula [36], the critical load of sandwich columns with egg honeycomb cores made by orthotropic faces is

$$P_I = \frac{2\pi^2}{3}\frac{wh_f^3}{a^2}E_f \tag{6}$$

For pyramidal honeycomb cores, simple elastic plate buckling theory can be used to derive an expression for the in-plane stress P_I in the skins at which intra-cell buckling occurs, the peak load being

$$P_I = \frac{4\sqrt{2}\pi^2}{3}\frac{wh_f^3}{a^2}E_f \tag{7}$$

3.1.4. Face sheet crushing

Since the three dimensional honeycomb core is much more compliant compared with face sheets, the face sheet crushing load can be estimated from,

$$P_{FY} = 2\sigma_{fy}h_f w \tag{8}$$

where σ_{fy} is the micro-buckling strength of the composite face sheet depending on the degree of fiber misalignment and the matrix shear strength. In the present study, σ_{fy} was obtained from compressive test of laminate.

3.1.5. Core member crushing

Honeycomb cores bear the compressive load with face sheet at the same time. The bearing capacity of face sheet is much higher than the honeycomb cores, thus the honeycomb cores will be crushed first at the low level load compared with the crushing failure of the face sheet, but the failure of honeycomb cores is not the dominated failure modes for the overall structures. The analytical peak load for the failure of egg and pyramidal honeycomb cores can be estimated with:

$$P_{CY} = \frac{m}{2}\sigma_s dh \tag{9}$$

where σ_s is the failure strength of honeycomb wall. For egg honeycomb cores, n is the number of slender laminate sheets in width direction $n = 2$.

$$P_{CY} = \frac{m}{2}dh\sigma_s \sin\omega \tag{10}$$

For pyramidal honeycomb cores, m is the number of slender laminate sheets in width direction $m = 6$.

Table 2
Mechanical properties of carbon fiber composite face-sheets and slender laminate sheets of honeycomb cores.

No.	Stack sequence	E_f (GPa)	σ_{fy} (MPa)	E_c (GPa)	σ_s (MPa)
(a)	$(0°/0°/0°/0°)_s$	100	850	54.504	473
(b)	$(0°/90°/90°/0°)_s$	54.504	473	54.504	473
(c)	$(90°/90°/90°/90°)_s$	8.4	96	54.504	473

3.2. Failure mechanism maps

In this section, we provide predictive failure maps for carbon fiber reinforced composite egg and pyramidal honeycombs core sandwich panels based on the above analytical parameters. The stacking sequence of the face sheets and the topology of honeycomb cores can have significant effect on the overall behavior and failure of composite sandwich panels. Results of sandwich columns failure in compression expressed in terms of maps facilitate visualization during the design stage. When constructing these maps, it was assumed that the operative failure mode was associated with the lowest critical load. These maps were developed as a function of the non-dimensional geometrical parameters h_f/H and L/H, and the boundaries of failure modes were obtained by equating the critical loads for different failure modes. In a previous work [39], we pointed out that the choice of parent material properties significantly influences the locations of the boundaries between failure modes for carbon fiber composite sandwich columns. For the laminate face-sheets with same thickness of single ply, the equivalent mechanical properties changed with different stack sequences; for the topologies of core, the equivalent shear modulus changed with different configurations. In order to explore this response, failure mechanism maps were constructed based on different laminate stack sequences and core configurations. The mechanical properties of carbon fiber composite face sheet with three different laminate stack sequences and the slender laminates sheets of honeycomb cores are listed in Table 2. The relevant failure mechanism maps are plotted in Fig. 5 for both egg and pyramidal honeycomb cores with three different designs.

In Fig. 5, it is possible to see that locations of boundaries between failure modes obviously change with different laminate stack sequences and core configurations. This indicates that the highest weight efficient sandwich structure can be obtained by changing the laminate stack sequence and truss core configuration. The designable characteristic of composite laminate and three dimensional honeycomb cores is another key advantageous feature of these panels.

4. Experimental results and discussion

Three sets of both topologies sandwich panels with different face sheet thickness, t_f, length, L and honeycomb thickness, d, were fabricated to explore the failure modes identified in Section 3. Table 3 shows the dimensions of each set of sandwich panels, as well as the analytical predictions for each failure mode and the measured peak load and the observed failure mode. In Table 3, the shear stiffness of egg and pyramidal honeycomb cores are G_c = 110 MPa and 190 MPa, respectively, which can be obtained from shear tests.

4.1. Specimen 1 (Egg and pyramidal honeycomb cores): Face wrinkling + Inter-cell buckling + Face crushing + core member crushing + core debonding

The measured compressive response of specimen 1 with [0°/90°/90°/0°] laminate sequence, including egg and pyramidal honeycomb cores (for egg honeycomb cores, L = 180.26 mm, h_f = 0.53 mm, w = 89.63 mm, $\bar{\rho} = 6.0\%$; for pyramidal honeycomb

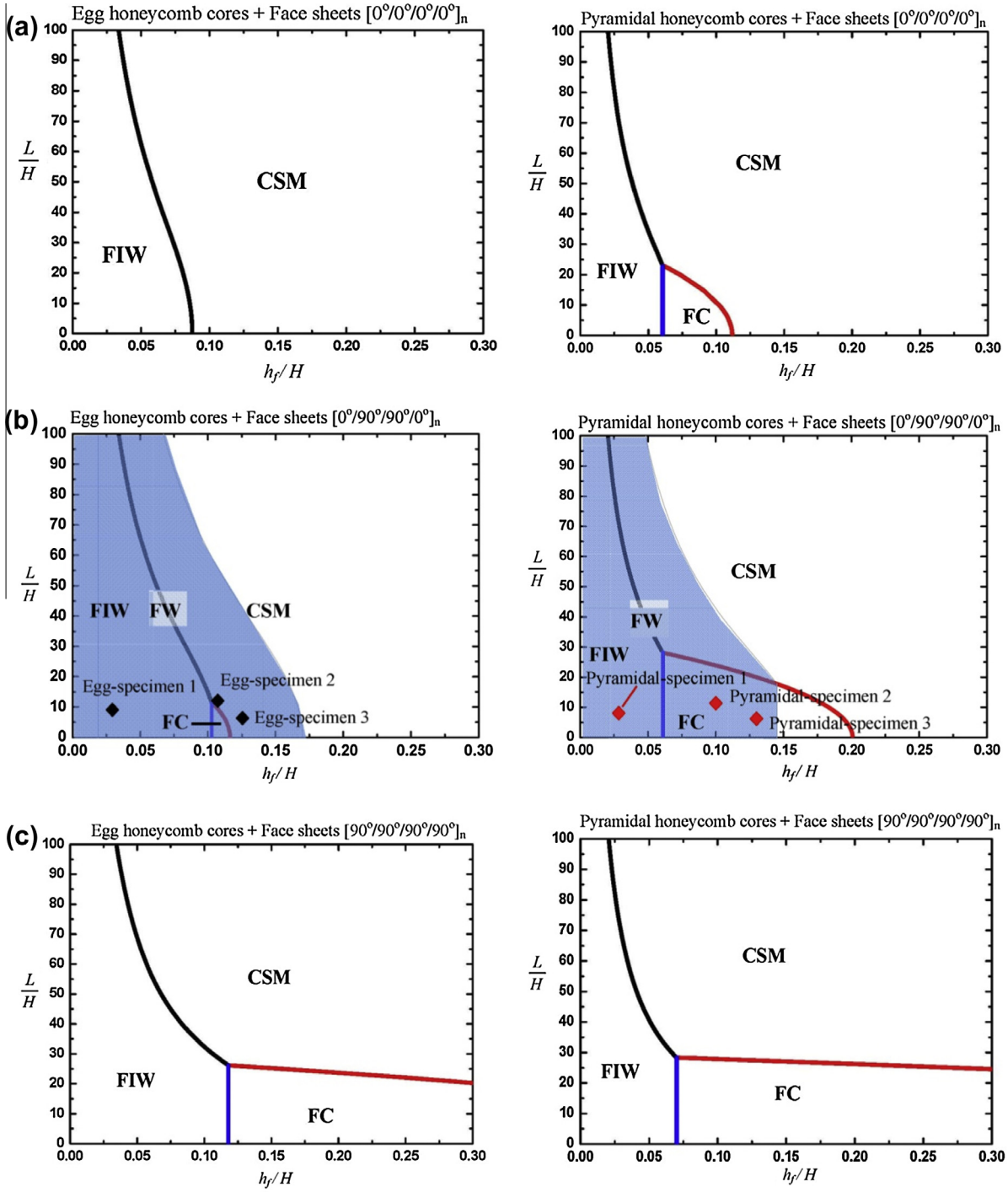

Fig. 5. Failure mechanism maps for carbon fiber composite sandwich panels with egg and pyramidal honeycomb cores under in-plane compression: FW = face sheet wrinkling; FIW = face sheet inter-cell wrinkling; FC = face sheet crushing; CSM = core shear macro-buckling. Three different sequencing of face sheets were considered and the middle face mechanism maps were used to design the specimens.

cores, $L = 158.78$ mm, $h_f = 0.52$ mm, $w = 94.58$ mm, $\bar{\rho} = 12.0\%$), is depicted in Fig. 6, along with a montage of photographs showing the specimen deformation and fracture at different stages of loading (I: face wrinkling, II: inter-cell buckling, III: debonding after buckling).

Fig. 6b shows the deformed configurations of the sandwich panel with egg honeycomb cores at different stages of loading. The load–displacement record is linear prior to wrinkling of the face sheets. This was followed by inter-cell buckling from the face sheet. Core crushing was also found in the experiments. Finally, core debonding occurred as the bonding layers were not strong enough to transmit the constraints of the egg honeycomb cores. The debonding occurred gradually between the egg honeycomb core and face sheets, leading to multiple drops in the load carrying capacity of the panel (stages III to IV). Fig. 6c shows the deformed configurations of the sandwich panel with pyramidal honeycomb cores at different stages of loading. Face wrinkling, inter-cell buckling, face crushing, core crushing and debonding were found in the experiments. All the failure processes of pyramidal honeycomb cores were similar to the processes found for egg honeycomb cores.

Table 3
Summary of the geometries employed in the end compression tests along with the predicted and measured failure loads and collapse modes.

Topology	Specimen number	L	h_f (mm)	w (mm)	t_c (mm)	$P_{pred.}$ (kN)	Analyt. fail.mode	$P_{obs.}$ (kN)	Obs. fail mode
Egg honeycomb cores	1	180.3	0.53	89.63	2.0	150.1 0.9 2.3 22.5 7.6	CSM FW FIW FC CC	10.4	FW/FIW/CC/CD
	2	224.2	2.07	89.67	2.0	175.5 55.0 137.7 175.6 7.6	CSM FW FIW FC CC	83.0	CC/CD/CSM
	3	132.5	2.51	89.38	2.0	189.8 97.8 244.7 212.2 7.6	CSM FW FIW FC CC	135.7	CC/CD/CSM
Pyramidal honeycomb cores	1	158.8	0.52	94.58	2.0	251.7 1.8 6.5 23.3 16.1	CSM FW FIW FC CC	15.0	FW/FIW/CC/FC/CD
	2	221.2	2.02	93.97	2.0	294.2 107.2 379.3 179.6 16.1	CSM FW FIW FC CC	121.2	CD/CSM
	3	126.1	2.52	94.32	2.0	339.5 208.9 739.1 224.9 16.1	CSM FW FIW FC CC	207.5	CD/FC

Where, P_{pred} = Prediction value of load P based on analytical equations, P_{obs} = Observed value of load P based on experimental results.

However, in pyramidal honeycomb cores, face crushing and core debonding were the dominant modes. It was found that the peak load of pyramidal honeycomb cores is larger than that of egg honeycomb cores due to the smaller wave length of pyramidal honeycomb cores between two unit cells. Therefore, buckling, which would induce debonding between honeycomb cores and face sheet, does not occur easily.

4.2. Specimen 2 (Egg and pyramidal honeycomb cores): Core shear macro-buckling + core member crushing + core debonding

Fig. 7a shows the response of specimen 2 with $[0°/90°/90°/0°]_4$ lamination sequence (for egg honeycomb cores, L = 224.18 mm, h_f = 2.07 mm, w = 89.67 mm, $\bar{\rho} = 6.0\%$; for pyramidal honeycomb cores, L = 221.2 mm, h_f = 2.02 mm, w = 93.97 mm, $\bar{\rho} = 12.0\%$). After the initial linear response, specimen 2 with egg honeycomb cores buckles and bends outward and the resisting force of the column decreases sharply. According to Eq. (4), the buckling load of the sandwich panel is $P_S \sim 175.493$ kN (note that for this sandwich panel $P_B \gg P_S$). The measured peak value is ~82.98 kN, about 53% lower than the theoretical prediction. The load–displacement curve drops sharply after core shear macro-buckling. The response of the panel at this stage of loading is governed by a combination of core shear buckling and debonding of the egg honeycomb cores from the face sheets as can be seen in Fig. 7b. The debonding occurs as the bonding between the core and face sheet is not strong enough to transfer the constraints of the cores. In addition to debonding, crushing of the egg honeycomb cores was also observed prior to the overall failure of the panel, as shown in Fig. 7b. Fig. 7c shows the deformation history of sandwich panels with pyramidal honeycomb cores. The load–displacement curves of pyramidal honeycomb cores are similar to egg honeycomb cores records except for the peak load which is larger than the previous value. The reason for that increase is the larger shear stiffness of pyramidal honeycomb cores in comparison with egg honeycomb cores. Debonding is also the dominating failure mode and both face sheets buckle and bend outward in opposite directions.

4.3. Specimen 3 (Egg and pyramidal honeycomb cores): Core shear macro-buckling + Face crushing + core member crushing + core debonding

According to the analytical study presented in Section 3.1, core shear buckling is the dominant elastic macro-buckling mode for sandwich panels with thick face sheets and long length of columns. Moreover, no practical laboratory scale column could be designed to study the Euler buckling mode. Two kinds of specimens with short length were designed to obtain face crushing. Fig. 8a shows the measured compressive response of specimen 3 with face sheets $[0°/90°/90°/0°]_5$ (for egg honeycomb cores, L = 132.54 mm, h_f = 2.51 mm, w = 89.38 mm, $\bar{\rho} = 6.0\%$; for pyramidal honeycomb cores, L = 126.05 mm, h_f = 2.52 mm, w = 94.32 mm, $\bar{\rho} = 12.0\%$). The peak load is larger for pyramidal honeycomb structures in comparison with egg honeycomb structures due to the different dominating failure mechanism. Fig. 8b shows the deformed configuration of the sandwich panel with egg honeycomb cores at different stages of deformation. The core shear macro-buckling observed can be attributed to the weak shear stiffness of egg honeycomb cores. Fig. 8c shows the deformed configuration of the sandwich panel with pyramidal honeycomb cores at different stages of deformation. In this experiment, a progressive face crushing was observed. As the compressive load reaches the critical load associated with the face crushing, both face sheets get crushed. Using the numerical method a value of σ_{fy} = 473 MPa was esti-

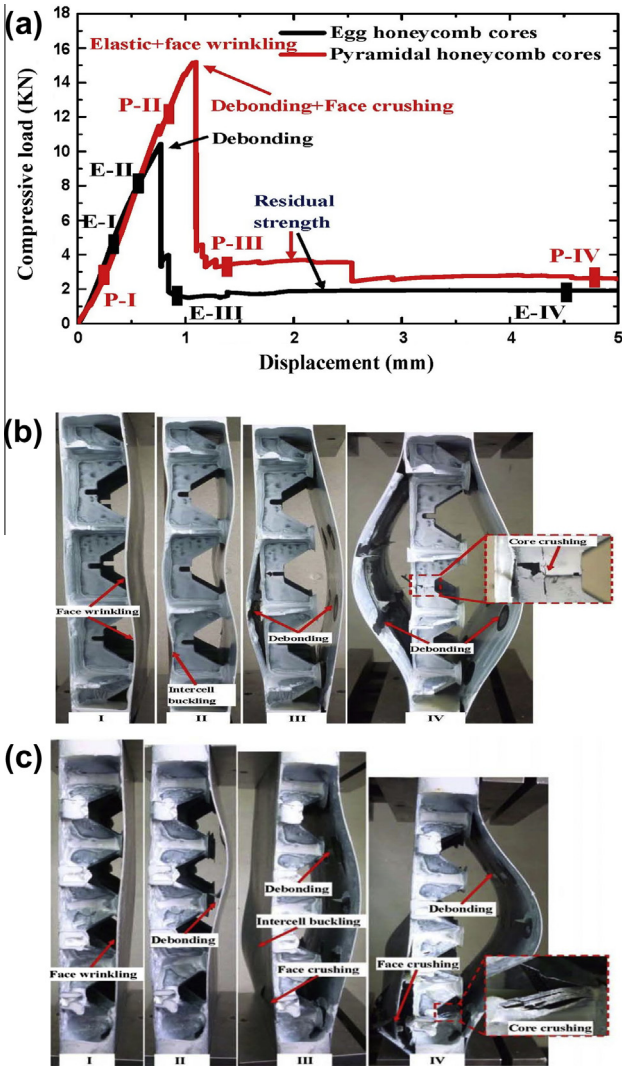

Fig. 6. Face wrinkling failure of sandwich panels with egg and pyramidal honeycomb cores (specimen 1). (a) Load–displacement curves, (b) photographs of the deformed panel at different stages of loading (E-I: Face wrinkling, E-II: face wrinkling and face inter-cell buckling, E-III: core debonding, E-IV: core debonding and core crushing). (c) An image of the deformed panel at different stages of loading (P-I: Face wrinkling; P-II: core debonding; P-III: core debonding, inter-cell buckling and face crushing; P-IV: core crushing after core debonding), showing the complete debonding of the face sheets from the core and outward buckling.

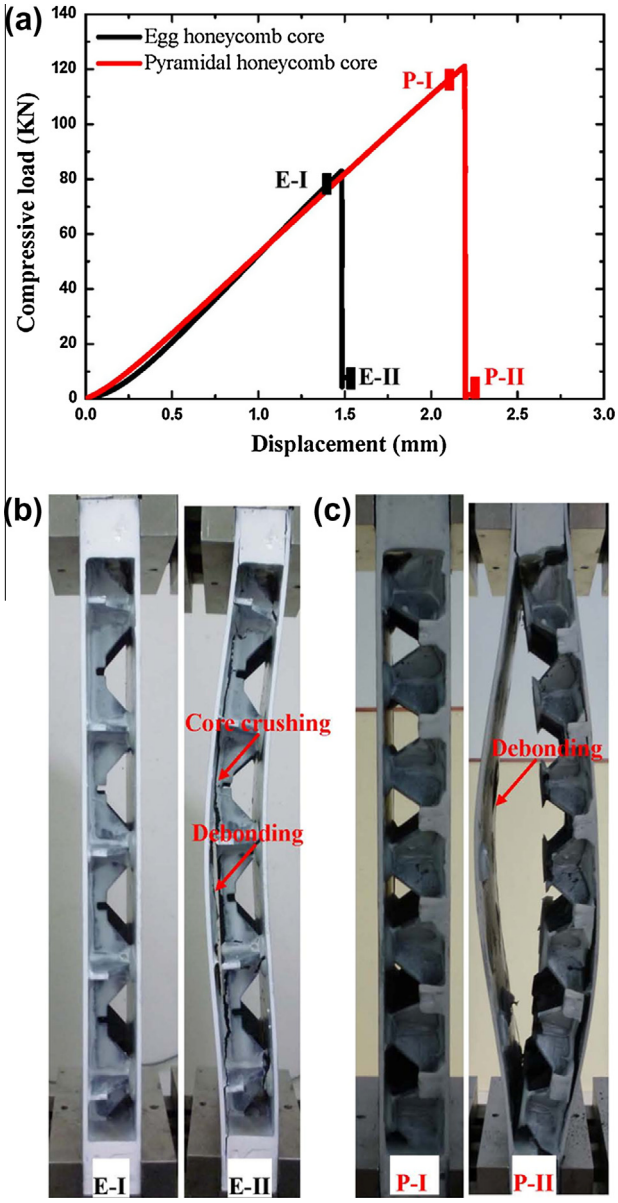

Fig. 7. Failure of sandwich panels with egg and pyramidal honeycomb cores (specimen 2). (a) Load–displacement curves, (b) photographs of the deformed panel at different stages of loading (E-I: before failure, E-II: after core shear macro-buckling). (c) An image of the deformed panel at different stages of loading (P-I: before failure, P-II: after core debonding), showing the complete debonding of the face sheets from the core and outward buckling.

mated for this panel configuration. The analytical estimate of the critical load based on Eq. (4) is about 212.2 kN. The measured peak value in Fig. 8a is 135.7 kN and is about 36% lower than the analytical prediction. This discrepancy is attributed to the imperfections in the manufactured specimens, as well as the assumptions made in developing the simple analytical model presented in Section 3 and in the estimation of micro-buckling strength of the composite face sheet. Local delamination of the face sheet near the clamped ends of the panel reduces the overall strength of the sandwich panel. The sandwich panel loses its integrity, as the core completely debonds from one of the face sheets, and each part of the panel bends outward.

5. Euler buckling failure and comparisons

No practical laboratory scale sandwich column could be designed to lie in the Euler buckling failure regime and thus this failure regime was not tested in above experimental study. A finite element method was used to investigate this failure mode. The sandwich columns with 3D honeycomb cores were made with T700/3234 composite materials and were meshed using ABAQUS software with fully integrated tetrahedron element with ideal elastic model. The homogeneous material properties are listed in Table 2. Surface to surface contact was used to model the contact between cores and face sheets. The buckling failure modes of both 3D honeycomb sandwich columns are sketched in Fig. 9. The comparisons of both 3D honeycomb cores with different geometries were also conducted based on the simulation model. The effect between span length and failure load are concluded in Fig. 10. It is assumed that $h_f = 2$ mm and $d = 2$ mm for both egg and pyramidal honeycomb cores The failure load decreases with the increasing span length, and the range between egg and pyramidal honeycomb cores becomes narrower with this increment. This is because the contribution of honeycomb core becomes smaller as the span in-

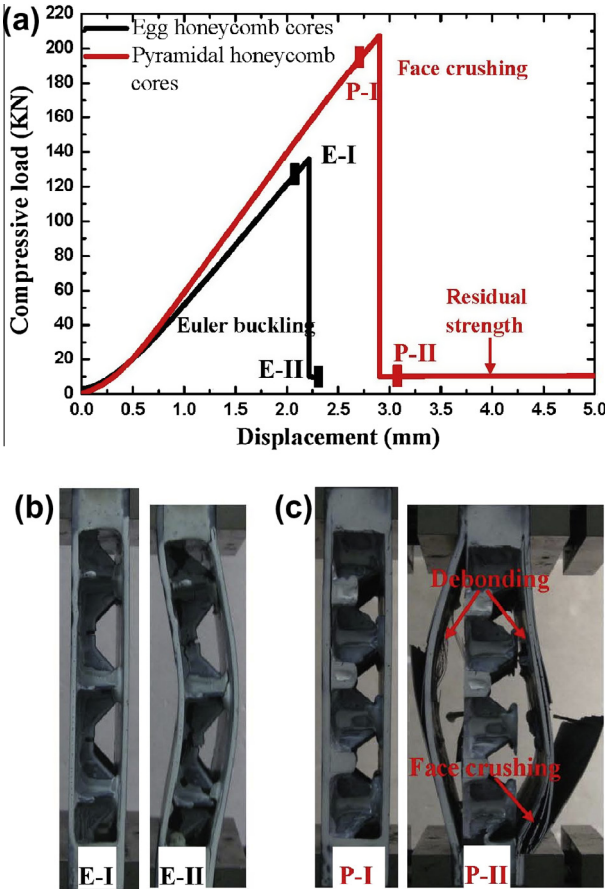

Fig. 8. Failure of sandwich panels with egg and pyramidal honeycomb cores (specimen 3). (a) Load–displacement curves, (b) photographs of the deformed panel at different stages of loading (E-I: before failure, E-II: after core shear macro-buckling). (c) An image of the deformed panel at different stages of loading (P-I: before failure, P-II: after face crushing and core debonding), showing the complete debonding of the face sheets from the core and outward buckling.

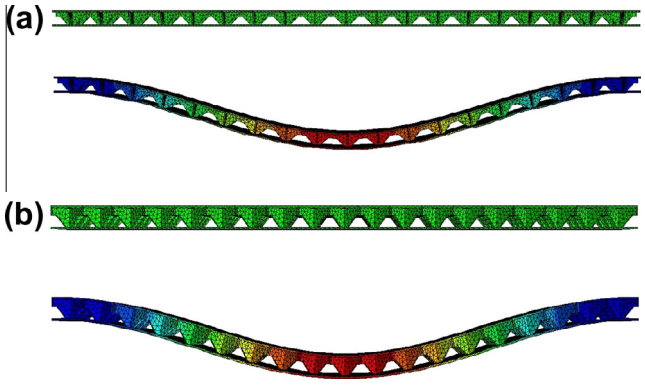

Fig. 9. Euler buckling failure for egg (a) and pyramidal (b) honeycomb sandwich columns done by simulation.

creases. Fig. 11 shows the relationship between failure load and the thickness of the facesheet. In this figure, the thickness of core wall is the same for both honeycomb cores, $d = 2$ mm. $L = 1001$ mm and 997.6 for egg and pyramidal honeycomb cores, respectively.

It was found that the range between two curves becomes wider with the increment of facesheet thickness due to the contribution of face sheet in the overall behavior. The relationship between the

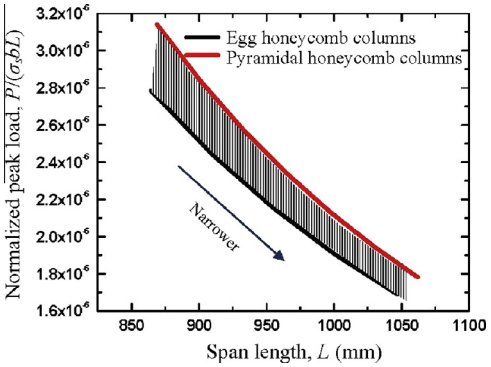

Fig. 10. The relationship between the normalized compressive peak loads of honeycomb sandwich columns and span length.

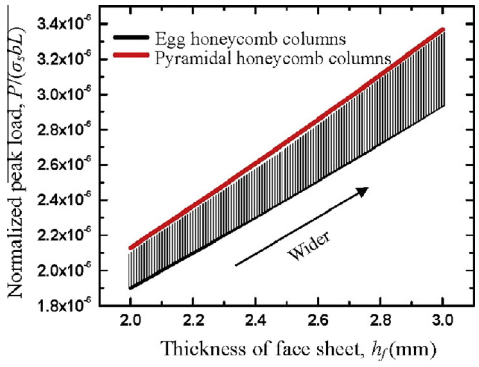

Fig. 11. The relationship between the normalized compressive peak loads of honeycomb sandwich columns and thickness of face sheet, h_f.

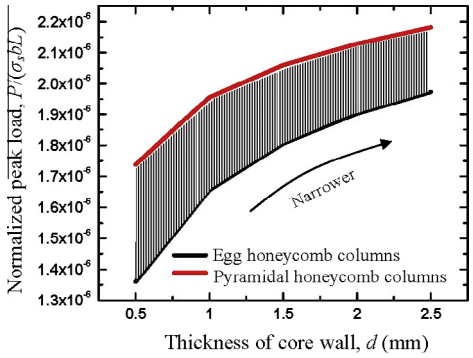

Fig. 12. The relationship between the normalized compressive peak loads of honeycomb sandwich columns and the thickness of core wall, d.

normalized compressive peak loads of honeycomb sandwich columns and the thickness of core wall is shown in Fig. 12. In this figure, the thickness of face sheet is the same for both honeycomb cores, $h_f = 2$ mm. $L = 1001$ mm and 997.6 for egg and pyramidal honeycomb cores, respectively. The value of failure load gets larger with the increasing of the thickness of core wall. However, the range between two curves becomes narrower since the contribution of failure load is dominated by length and the ratio of contribution for core wall is very limited. It can be concluded that the mechanical properties of pyramidal honeycomb sandwich columns are much better than that of the egg honeycomb sandwich column. The results from simulation have a good agreement with the analytical predictions.

6. Conclusions

A series of analytical, experimental and numerical investigations were conducted to study the response and failure of 3D honeycomb core sandwich panels with through-inner spaces made of carbon fiber composite under in-plane compression. In the analytical part of the study, several failure modes as Euler or core shear macro-buckling, face wrinkling, face sheet crushing, core member crushing and face inter-cell buckling were considered and theoretical relationships for predicting the failure load associated with each mode were presented. The failure mechanism maps were constructed in order to predict the failure modes with different structural parameters. In the experimental part of the study, Three different sets of specimens with egg and pyramidal honeycomb cores were manufactured to study the failure modes, Face wrinkling, inter-cell buckling, core shear macro-buckling, face crushing, core member crushing and core debonding have been observed. Simulation works were conducted in order to predict the failure of Euler buckling, The relationship between the normalized compressive peak loads of honeycomb sandwich columns and span length, thicknesses of face sheet and core wall have been also addressed. The mechanical properties of pyramidal honeycomb sandwich columns are much better than that of the egg honeycomb sandwich column.

Acknowledgements

The present work was supported in part by the Major State Basic Research Development Program of China (973 Program) under Grant No. 2011CB610303, National Science Foundation of China under Grant Nos. 11222216, 11302060 and the Fundamental Research Funds for Central Universities under Grant No. HIT.BRETIV.201301. JX also gratefully acknowledges Supported by Natural Scientific Research Innovation Foundation in Harbin Institute of Technology (HIT.NSRIF.2014025) and the National Key Lab of Materials and Structures in Special Environment.

References

[1] He L, Cheng YS, Liu J. Precise bending stress analysis of corrugated-core, honeycomb-core and X-core sandwich panels. Compos Struct 2012;94:1656–68.
[2] Qin QH, Wang TJ. Low-velocity impact response of fully clamped metal foam core sandwich beam incorporating local denting effect. Compos Struct 2013;96:346–56.
[3] Wang ZG, Tian HQ, Lu ZJ, Zhou W. High-speed axial impact of aluminum honeycomb-experiments and simulations. Compos Part B 2014;56:1–8.
[4] Vaziri A, Xue ZY. Mechanical behavior and constitutive modeling of metal cores. J Mech Mater Struct 2007;2:1743–60.
[5] Tan ZH, Luo HH, Long WG, Han X. Dynamic response of clamped sandwich beam with aluminium alloy foam core subjected to impact loading. Compos part B:Eng. 2013;46:39–45.
[6] Jing L, Wang ZH, Ning JG, Zhao LM. The dynamic response of sandwich beams with open-cell metal foam cores. Compos Part B: Eng 2011;42(1):1–10.
[7] Lee BK, Kang KJ. Compressive strength of tube-woven Kagome truss cores. Script Mater 2009;60:391–4.
[8] Gordon LM, Bouwhuis BA, Suralvo M, McCrea JL, Palumbo G, Hibbard GD. Micro-truss nanocrystalline Ni hybrids. Acta Mater 2009;57:932–9.
[9] Jacobsen AJ, Carter WB, Nutt S. Compression behavior of micro-scale truss structures formed from self-propagating polymer waveguides. Acta Mater 2007;55:6724–33.
[10] Moongkhamklang P, Deshpande VS, Wadley HNG. The compressive and shear response of titanium matrix composite lattice structures. Acta Mater 2010;58:2822–35.
[11] Chen Z, Yan N. Investigation of elastic moduli of Kraft paper honeycomb core sandwich panels. Compos Part B 2012;43(5):2107–14.
[12] Xiong J, Ma L, Wu LZ, Wang B, Vaziri A. Fabrication and crushing behavior of low density carbon fiber composite pyramidal truss structures. Compos Struct 2010;92(11):2695–702.
[13] Finnegan K, Kooistra G, Wadley HNG, Deshpande VS. The compressive response of carbon fiber composite pyramidal truss sandwich cores. Int J Mater Res 2007;98(12):1264–72.
[14] Ashby MF. Materials selection in mechanical design. 4th ed. Boston: A Butterworth-Heinemann; 2010.
[15] Joo JH, Kang KJ, Kim T, Lu TJ. Forced convective heat transfer in all metallic wire-woven bulk Kagome sandwich panels. Int J Heat Mass Trans 2011;54:5658–62.
[16] Ebrahimi H, Vaziri A. Metallic sandwich panels subjected to multiple intense shocks. Int J Solids Struct 2013;50:1164–76.
[17] Vaziri A, Hutchinson JW. Metallic sandwich plates subject to intense air shocks. Int J Solids Struct 2007;44:2021–35.
[18] Xin FX, Lu TJ. Analytical modeling of fluid loaded orthogonally rib-stiffened sandwich structures: sound transmission. J Mech Phys Solids 2010;58:1374–96.
[19] Xin FX, Lu TJ. Sound radiation of orthogonally rib-stiffened sandwich structures with cavity absorption. Compos Sci Technol 2010;70:2198–206.
[20] Fan HL, Meng FH, Yang W. Sandwich panels with Kagome lattice cores reinforced by carbon fibers. Compos Struct 2007;81:533–9.
[21] Fan HL, Yang L, Sun FF, Fang DN. Compression and bending performances of carbon fiber reinforced lattice-core sandwich composites. Compos Part A 2013;52:118–25.
[22] Zheng JJ, Zhao L, Fan HL. Energy absorption mechanisms of hierarchical woven lattice composites. Compos Part B 2012;43(3):1516–22.
[23] Zheng Q, Fan HL, Liu J, Ma Y, Yang L. Hierarchical lattice composites for electromagnetic and mechanical energy absorptions. Compos Part B 2013;53:152–8.
[24] Russell BP, Deshpande VS, Wadley HNG. Quasistatic deformation and failure modes of composite square honeycomb. J Mech Mater Struct 2008;3:1315–40.
[25] Russell BP, Liu T, Fleck NA, Deshpande VS. The soft impact of composite sandwich beams with a square-honeycomb core. Int J Impact Eng 2012;48:65–81.
[26] Park S, Russell BP, Deshpande VS, Fleck NA. Dynamic compressive response of composite square honeycombs. Compos Part A 2012;43:527–36.
[27] Ajdari A, Jahromi BH, Papadopoulos J, Vaziri A. Hierarchical honeycombs with tailorable properties. Int J Solids Struct 2012;49:1413–9.
[28] Ajdari A, Hashemi HN, Vaziri A. Dynamic crushing and energy absorption of regular, irregular and functionally graded cellular structures. Int J Solids Struct 2011;48:506–16.
[29] Petrone G, Rao S, Rosa SD, Mace BR, Franco F, Bhattacharyya D. Initial experimental investigations on natural fibre reinforced honeycomb core panels. Compos Part B 2013;55:400–6.
[30] Jang TS, Oh DS, Kim JK, Kang KI, Cha WH, Rhee SW. Development of multi-functional composite structures with embedded electronics for space application. Acta Astron 2011;68:240–52.
[31] Hou SJ, Li Q, Long SY, Yang XJ, Li W. Design optimization of regular hexagonal thin-walled columns with crashworthiness criteria. Finite Elements Analys Des 2007;43:555–65.
[32] Xiong J, Ma L, Stocchi A, Yang JS, Wu LZ, Pan SD. Bending response of carbon fiber composite sandwich beams with three dimensional honeycomb cores. Compos Struct 2014;108:234–42.
[33] Xiong J, Ma L, Wu LZ, Liu JY, Vaziri A. Mechanical behavior and failure of carbon fiber composite pyramidal truss core sandwich columns. Compos Part B 2011;42:938–45.
[34] Li M, Wu LZ, Ma L, Wang B, Guan ZX. Structural response of all-composite pyramidal truss core sandwich columns in end compression. Compos Struct 2011;93:1964–72.
[35] Cote F, Biagi R, Smith HB, Deshpande VS. Structural response of pyramidal core sandwich columns. Int J Solids Struct 2007;44:3533–56.
[36] Carlsson LA, Kardomateas GA. Structural and failure mechanics of sandwich composites. Dordrecht Heidelberg, London, New York: Springer; 2011.
[37] Allen HG. Analysis and design of structural sandwich panels. New York: Pergamon Press; 1969.
[38] Fleck NA, Sridhar I. End compression of sandwich columns. Compos Part A 2002;33:353–9.
[39] Xiong J, Ma L, Pan SD, Wu LZ, Papadopoulos J, Vaziri A. Shear and bending performance of carbon fiber composite sandwich panels with pyramidal truss cores. Acta Mater 2012;60:1455–66.